Thermal and Mechanical Controls on the Evolution of Archean Crustal Deformation: Examples From Western Australia

Simon Bodorkos and Mike Sandiford

School of Earth Sciences, University of Melbourne, Victoria, Australia

Dome-and-keel formation in Archean granite–greenstone terrains was uniquely favored by high abundances of heat-producing elements (HPEs) in the crust, and the ubiquity of pre-doming "greenstone-over-granite" stratification, which constituted large-scale density inversions and facilitated long-term steepening of the geotherm via burial of felsic basement-hosted HPEs. This contribution investigates the influence of these factors on the thermo-mechanical stability of the crust, with reference to two contrasting Archean granite–greenstone terrains in Western Australia. In the Neoarchean Eastern Goldfields Province, the rapid (2715–2665 Ma) accumulation of a thin (8-km) greenstone succession atop HPE-poor felsic crust (radiogenic heat flow contribution $q_c = 45$ mW m^{-2}) raised mid-crustal temperatures from 230 °C to 370 °C prior to 2650 Ma dome-and-keel formation. In such cold, strong crust, the development of broad, granite-cored antiforms and narrow, greenstone-cored synforms with little strike variation is likely to directly reflect far-field, horizontal tectonic forces, oriented perpendicular to the regional structural grain. In contrast, the Mesoarchean East Pilbara Granite–Greenstone Terrane underwent slow (3515–3325 Ma) accumulation of tick (14-km) greenstones atop HPE-rich ($q_c = 70$ mW m^{-2}) basement, which raised mid-lower crustal temperatures from 400 °C to 750–800 °C, prior to 3300 Ma dome-and-keel formation. The effective viscosity of this hot, weak crust was further reduced by partial melting of the felsic basement; the resulting "classical" architecture (featuring granite domes flanked by greenstone keels with a variety of strike orientations) may therefore reflect partial convective overturn and vertical reorganization of the crust during thermo-mechanical stabilization.

INTRODUCTION

"Dome-and-keel" structure is a distinctive feature of Archean granite–greenstone terrains worldwide. In general, variably deformed and metamorphosed granitoids define broad, high-amplitude "domes" that are separated from each other by narrow, synformal "keels" consisting of steeply dipping supracrustal greenstone successions [e.g., *Macgregor*, 1951; *Anhaeusser et al.*, 1969; *Hickman*, 1983, 1984; *Marshak et al.*, 1992, 1999; *Choukroune et al.*, 1995, 1997; *Chardon et al.*, 1998; *Collins et al.*, 1998; *Van Kranendonk et al.*, 2004]. This crustal architecture reflects the prevalence of a peculiarly Archean phenomenon: the widespread early development of a gross tectono-stratigraphy comprising one or more relatively dense supracrustal successions (dominated by mafic and ultramafic volcanic rocks) overlying less-dense felsic crust of tonalite–trondhjemite–granodiorite (TTG) composition [e.g., *de Wit and Ashwal*, 1997; *Bleeker*, 2002; *Sandiford et al.*, 2004; and references therein]. In detail, Archean dome-and-keel provinces may be divided into two major groups, based primarily on the first-order

Archean Geodynamics and Envionments
Geophysical Monograph Series 164

structural geometry of the upper and middle crust [e.g., *Peschler et al.*, 2004], but also encapsulating important differences in age and tectono-magmatic relationships.

The first group comprises predominantly Mesoarchean (3.5–3.0 Ga) terrains featuring "classical" architecture. Curviplanar greenstone keels with short strike lengths and a wide range of strike orientations typically flank and separate several relatively large domal granitoid complexes (50–90-km diameter in plan view). In most cases, episodic but voluminous felsic magmatism (in the form of granite plutonism in dome cores and coeval, thick volcanic intercalations within overlying supracrustal successions) played an active role in the formation and amplification (or inflation) of dome-and-keel structure over an extended period (>500 My). Examples include the Zimbabwe Craton [e.g., *Macgregor*, 1951; *Anhaeusser et al.*, 1969; *Jelsma et al.*, 1993], the eastern Pilbara Craton (Figure 1b) of Western Australia [e.g., *Hickman*, 1983, 1984; *Van Kranendonk et al.*, 2002], and the western Dharwar Craton of southern India [e.g., *Choukroune et al.*, 1995, 1997; *Chardon et al.*, 1996, 2002].

In contrast, the second group is dominated by Neoarchean terrains (post 3.0 Ga, and mostly 2.75–2.65 Ga) and are typified by granitoid domes of widely varying shape and size, though domes with well-developed outlines tend to be pseudo-elliptical in plan view. These granitoids occur as antiformal culminations enveloped by laterally extensive greenstone belts, with long strike lengths and little variation in strike orientation. Felsic magmatism was relatively short-lived (<100 My), and mostly predated large-scale dome-and-keel amplification. The resulting map patterns resemble (at least superficially) those of post-Archean orogenic belts, and examples include the Eastern Goldfields Province (Figure 1c) of the Yilgarn Craton, Western Australia [e.g., *Griffin*, 1990; *Swager et al.*, 1997; *Krapez et al.*, 2000; *Blewett et al.*, 2004a; *Goleby et al.*, 2004], and the western Superior Province of Canada [e.g., *Card*, 1990; *Henry et al.*, 2000; *Thurston*, 2002; *Tomlinson et al.*, 2003; *White et al.*, 2003; *Percival et al.*, 2004].

Notwithstanding the existence of some notable exceptions to the above generalizations, the potential reasons for these apparent secular contrasts in the timing, duration, and nature of the interplay between large-scale upper-crustal deformation and felsic magmatic activity remain poorly understood [e.g., *Choukroune et al.*, 1997; *Bleeker*, 2002]. Do the observed patterns reflect a secular Archean evolution of tectonic processes [e.g., *Hamilton*, 1998], an evolving response of the Archean crust and upper mantle lithosphere to essentially time-invariant tectonic processes [e.g., *de Wit*, 1998], or some combination of the two? Could the relationship between deformation pattern and age reflect some systematic bias in the preserved record of Archean granite–greenstone terrains [*Morgan*, 1985]? It is likely that the answers to these questions are linked and reflect an important feedback between the physical properties of the Archean lithosphere, the nature of tectonic processes that shape it, and the tendency of those processes to stabilize (and therefore preserve) cratonic nuclei.

The primary aims of this paper are to explore the potential link between syn-tectonic thermal regimes and the styles of crustal-scale deformation in Archean granite–greenstone terrains and to examine how this relationship may have changed through time. We commence with a brief review of the factors exerting long-term influence on the thermal evolution of a typical Archean greenstone-over-granite crust, with emphasis on the abundance (q_c) and depth distribution (z_c) of crustal heat production, and the deep mantle heat flux (q_m; see next section). This is followed by a geological overview of two West Australian (Figure 1a) granite–greenstone terrains [the Mesoarchean East Pilbara Granite–Greenstone Terrane (Figure 1b) and the Neoarchean Eastern Goldfields Province (Figure 1c)] that are characterized by broadly comparable histories of greenstone accumulation atop ancient felsic basement but disparate dome-and-keel morphology. In each terrain, the available stratigraphic, structural, geophysical, geochemical, and geochronological constraints are used to estimate syn-tectonic q_c, z_c, and q_m values and to formulate simplified (one-dimensional) greenstone accumulation histories. These data are used as input for thermal models of each terrain, aimed at quantifying the potential extent of mid-crustal heating (attributable to the burial of relatively HPE-rich felsic crust beneath insulating greenstones) and the potential influence of such heating on the effective viscosity (and therefore mechanical behavior) of the mid-crust in each case. Finally, we consider the feedback relations affecting the thermo-mechanical behavior of the Archean crust and upper lithosphere in terms of the potential for secular change in both the processes governing crustal deformation and the record of those processes preserved by granite–greenstone terrains.

THERMAL CONSEQUENCES OF A REVERSE-STRATIFIED ARCHEAN CRUST

Most Archean granite–greenstone terrains were characterized by two fundamental crustal properties that incontrovertibly favored dome-and-keel formation. Firstly, granitic rocks comprised 50–60% of the crust, and their concentrations of the radioactive heat-producing elements (HPEs) K, Th, and U were at least two to three times higher than at present [e.g., *Pollack*, 1997]. Secondly, the early stages of crustal growth and active tectonism typically resulted in the widespread development of greenstone-over-granite tectono-stratigraphy [e.g., *Bleeker*, 2002]. This combination of properties had two

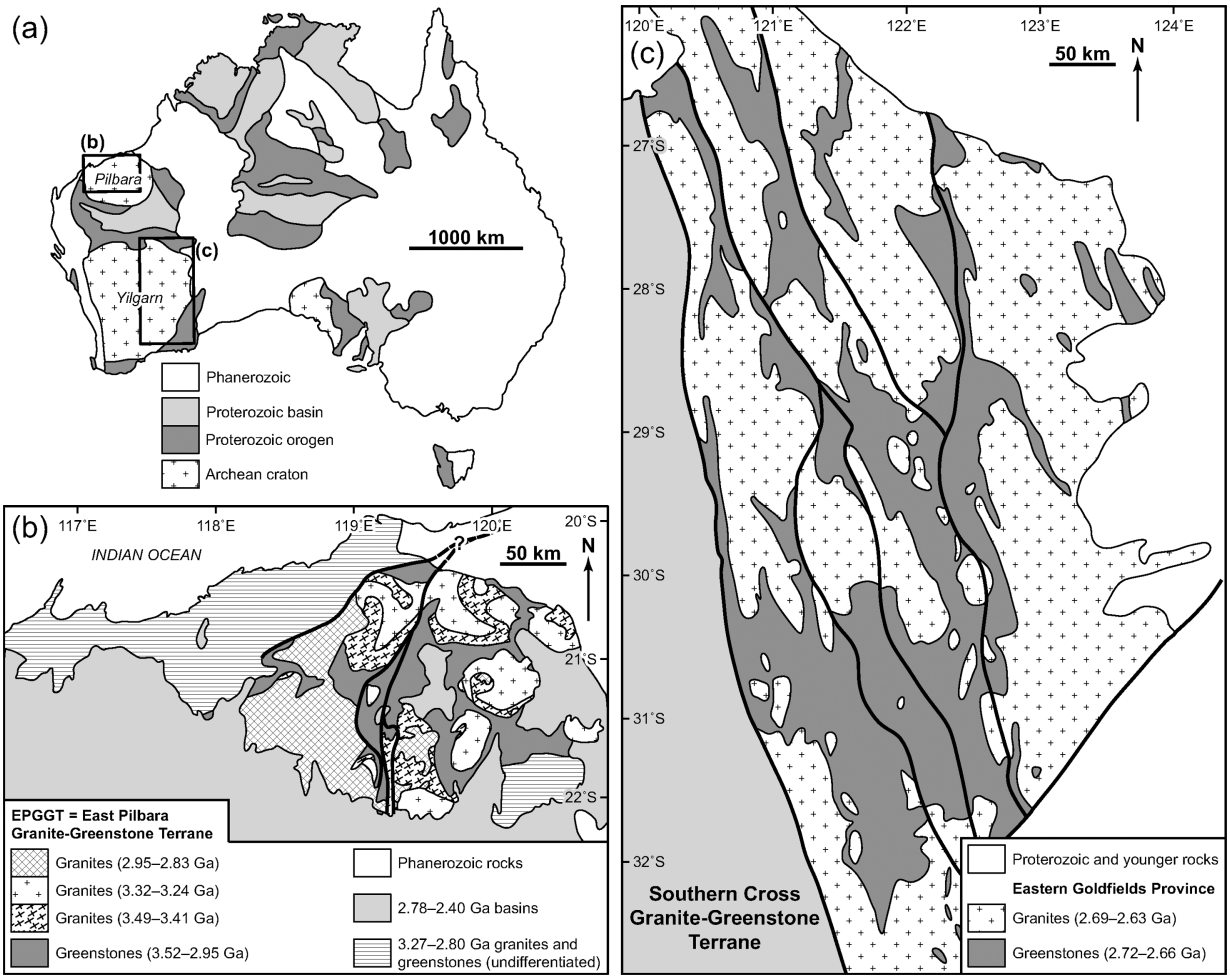

Figure 1. (a) Precambrian tectonic elements of Australia (modified after *Myers et al.* [1996]), showing the areas of the Archean cratons that form the focus of this study. Note that (b) and (c) have a common scale. (b) The Mesoarchean East Pilbara Granite–Greenstone Terrane (modified after *Van Kranendonk et al.* [2002] and *Hickman and Van Kranendonk* [2004]). Granite domes are typically pseudo-circular in plan view and separated from each other by greenstone keels with a variety of strike orientations. (c) The Neoarchean Eastern Goldfields Province (modified after *Myers* [1997] and *Blewett et al.* [2004a]). In plan view, granite domes are elongated parallel to the NNW–SSE structural grain, and there is little strike variation within the greenstone keels.

important thermo-mechanical consequences: (1) A substantial gravitational instability was generated by the density inversion within the reverse-stratified crust [e.g., *Mareschal and West*, 1980; *Collins et al.*, 1998; *de Bremond d'Ars et al.*, 1999], and (2) significant long-term steepening of the geotherm (termed "conductive incubation" by *Sandiford et al.* [2004]) occurred as a direct result of the burial of HPE-rich felsic crust beneath a thick greenstone edifice [see also *West and Mareschal*, 1979; *Ridley and Kramers*, 1990; *Sandiford and McLaren,* 2002; *Pysklywec and Beaumont*, 2004].

In the absence of significant advection, one-dimensional (vertical) heat flow at the Earth's surface (q_s) may be approximated by the sum of two independent components: "deep" conductive heating driven by asthenospheric convection (q_m), and "shallow" radiogenic heating controlled by the abundance (q_c) of predominantly crust-hosted HPEs:

$$q_s = q_m + q_c \quad (1)$$

The one-dimensional geotherm, $T(z)$, where z is depth, is governed by a similar relationship:

$$T(z) = T_m(z) + T_c(z) \quad (2)$$

For the syn-tectonic greenstone-over-granite tectonostratigraphy characteristic of most Archean granite–greenstone

terrains, the vertical distribution of HPEs may be approximated (in one dimension) by a three-layer configuration. This typically consists of a greenstone layer (of thickness z_1 and negligible HPE content), overlying a TTG layer (of thickness z_2-z_1 and depth-independent volumetric heat production H), which in turn overlies a lower crust and conductive lithosphere with zero HPE content. Assuming a constant deep mantle heat flux q_m at the base of the conductive lithosphere and a uniform, temperature-independent thermal conductivity (k) within the lithosphere, the steady-state geotherm is given by *Sandiford et al.* [2004]:

$$T(z) = \frac{q_m}{k} z + \left[\frac{H(z_2 - z_1)}{k} \right] z \quad 0 < z < z_1 \tag{3a}$$

$$T(z) = \frac{q_m}{k} z + \left[\frac{H(2z_2 - z)}{2k} \right] z - \frac{Hz_1^2}{2k} \quad z_1 < z < z_2 \tag{3b}$$

$$T(z) = \frac{q_m}{k} z + \frac{H(z_2^2 - z_1^2)}{2k} \quad z > z_2 \tag{3c}$$

Beneath the base of the heat-producing crust (i.e., for $z > z_2$), the maximum crustal contribution to the geotherm (i.e., the second term of equation (3c)) is independent of z [*Sandiford et al.*, 2002], and is denoted T_c'. *Sandiford and McLaren* [2002] showed that T_c' may be re-expressed in terms of the depth-integrated heat production (equivalent to q_c) and the characteristic depth of the heat production distribution (z_c). In the scenario described above, q_c is given by:

$$q_c = \int_{z_1}^{z_2} H dz = H(z_2 - z_1) \tag{4a}$$

and z_c corresponds to the depth-midpoint of the TTG layer:

$$z_c = z_1 + \frac{z_2 - z_1}{2} = \frac{z_1 + z_2}{2} \tag{4b}$$

Substituting equations (4a) and (4b) into the expression for T_c' within equation (3c) gives:

$$T_c' = \frac{q_c z_c}{k} \tag{5}$$

The sensitivity of deep crustal temperatures to q_c and q_m is well understood, but equation (5) highlights the additional importance of z_c. Its influence is illustrated by considering the long-term thermal evolution of the material point corresponding to the base of the TTG layer, following an instantaneous increase (Δz) in the thickness of the supracrustal greenstone layer (without altering z_2-z_1, H, or q_m). The initial temperature at $z = z_2$ is given by equation (3c):

$$T(z_2) = \frac{q_m z_2 + q_c z_c}{k} \tag{6a}$$

Following greenstone emplacement (and subsequent thermal equilibration), the temperature at the base of the TTG layer is given by:

$$T(z_2 + \Delta z) = \frac{q_m (z_2 + \Delta z) + q_c (z_c + \Delta z)}{k} \tag{6b}$$

Subtracting (6b) from (6a), the long-term temperature increase (ΔT) is:

$$\Delta T = \frac{\Delta z (q_m + q_c)}{k} \tag{7}$$

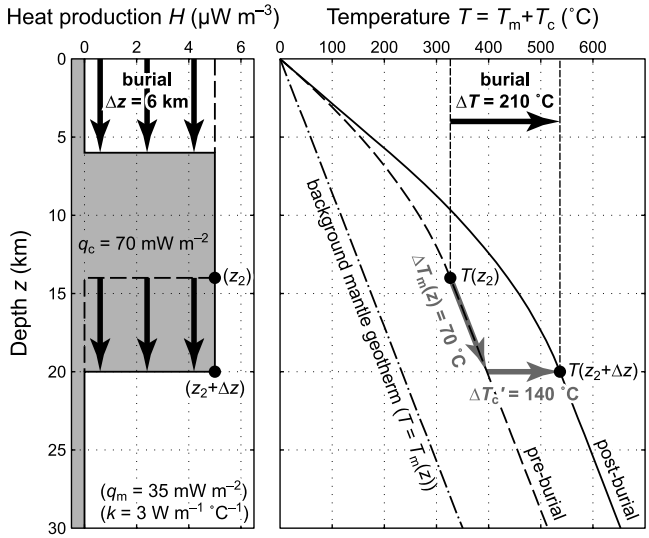

Figure 2. Steepening of the ambient geotherm as a consequence of the burial of HPE-rich felsic crust beneath a greenstone edifice. In the left panel, burial associated with greenstone accumulation is indicated by the thick black arrows; the unfilled dashed outline and the gray-filled solid outline correspond to the pre- and post-burial depth distributions, respectively, of HPEs. The right panel shows the time-invariant "mantle" component of the geotherm ($T_m(z)$), the pre-burial geotherm, and the post-burial geotherm, assuming that thermal equilibrium has been attained. The black circle (corresponding to the base of the heat-producing layer) has undergone a temperature increase of 210 °C during burial, only one-third of which is due to migration down the mantle geotherm ($\Delta T_m(z)$); the remainder ($\Delta T_c'$) is independent of z and is due to conductive incubation resulting from deepening of HPEs [e.g., *Sandiford et al.*, 2002].

The significance of equation (7) is realized with the appreciation that the magnitude of q_c may have been as much as twice that of q_m in the Archean Earth, due to the abundance of HPEs [*Sandiford et al.*, 2004]. This is best illustrated by example (Figure 2): The emplacement of a 6-km-thick greenstone succession atop an Archean terrain with TTG-hosted $q_c = 70$ mW m^{-2} and $q_m = 35$ mW m^{-2} translates to a long-term temperature *increase* $\Delta T = 210$ °C at the base of the heat-producing crust (Figure 2). Two-thirds of this increase is directly attributable to conductive incubation via the burial of HPEs ($\Delta T_c' = 140$ °C; Figure 2); the remainder is due to migration of the base of the heat-producing crust down the mantle geotherm ($\Delta T_m(z) = 70$ °C; Figure 2), defined by the first term in each of equations (3a)–(3c).

However, the rate of deep crustal heating is dictated by the thermal response time of the lithosphere, so the magnitude of ΔT also depends upon the extent of thermal equilibration within the greenstone-over-granite stratified crust, prior to significant external modification via erosion, deformation, and/or magmatism. In the next section, we summarize the geology of the Mesoarchean East Pilbara Granite–Greenstone Terrane and the Neoarchean Eastern Goldfields Province, with emphasis on the stratigraphic and geochronological constraints on the nature, timing, and extent of greenstone accumulation. This provides a basis for quantitative assessment of the changes in the thermal structure of the crust prior to dome-and-keel formation.

GEOLOGICAL OVERVIEW

The East Pilbara Granite–Greenstone Terrane and the Eastern Goldfields Province (hereafter referred to as the Pilbara and the Goldfields, respectively) display several lithologic and tectono-stratigraphic similarities, despite significant differences in the timing and style of crustal growth and deformation. Both are characterized by the early development of regional greenstone-over-granite stratification [*Swager*, 1997; *Krapez et al.*, 2000; *Van Kranendonk et al.*, 2002] and an upper crust comprising felsic-dominated plutonic rocks and mafic-dominated volcanic rocks in roughly equal proportions by volume [*Wellman*, 2000; *Goleby et al.*, 2004]. In addition, both preserve isotopic evidence for the widespread existence of felsic crust that is considerably older than the exposed granites: *Smithies et al.* [2003] obtained 48 pre-3450 -Ma Nd model ages from 50 Pilbara granites with magmatic (U–Pb zircon) ages in the range 3450–2850 Ma, and *Champion and Sheraton* [1997] demonstrated that Nd model ages are at least 100 My older than magmatic crystallization ages for granites throughout the Goldfields.

Pilbara

The oldest exposed greenstone succession is the 3515–3495 Ma Coonterunah Group [*Buick et al.*, 1995], which locally reaches 6 km in thickness [*Green et al.*, 2000] and is overlain by the regionally extensive 3490–3425 Ma lower Warrawoona Group, which is up to 10–12 km thick [*Hickman*, 1983; *Van Kranendonk et al.*, 2002]. Plutonic rocks of TTG composition were episodically emplaced into the lower parts of the both successions over the interval 3490–3410 Ma, and granite–greenstone contacts are intrusive and/or sheared. After an extended (70–80 My) hiatus, the 3350–3325 Ma upper Warrawoona Group, which is up to 8 km thick [*Van Kranendonk et al.*, 2002; *Bagas et al.*, 2004], was deposited atop the pre-3425 Ma crust. It is therefore likely that the regional stratigraphic thickness of the greenstone edifice was approximately 11–17 km, prior to the first major episode of dome-and-keel formation at ca. 3300 Ma [*Sandiford et al.*, 2004].

Dome-and-keel formation was accompanied by voluminous granitic magmatism in the easternmost Pilbara [e.g., *Williams and Collins*, 1990; *Barley and Pickard*, 1999], although the means of dome-and-keel formation remains the subject of considerable debate. Granite ascent through the overlying greenstones was initially attributed to solid-state diapirism [*Hickman*, 1983, 1984], but more recent interpretations of the granite domes include (1) magmatic diapirism and gravity-driven partial convective overturn of the crust [e.g., *Collins*, 1989; *Collins et al.*, 1998; *Van Kranendonk et al.*, 2002, 2004], (2) steepened metamorphic core complexes unroofed via extension of the overlying greenstones [e.g., *Zegers et al.*, 1996; *Kloppenburg et al.*, 2001], and (3) granite-cored antiformal culminations produced by complex cross-folding [e.g., *Blewett*, 2002, 2004b].

Goldfields

Pre-doming greenstones in the Goldfields are characterized by a relatively restricted range of ages. With the exception of the southwesternmost Goldfields (where a package of ca. 2900 Ma mafic volcanic rocks up to 1–2 km in thickness is locally exposed [*Nelson*, 1997; *Swager*, 1997]), the volcanosedimentary successions were deposited over the 50My interval 2715–2665 Ma [*Brown et al.*, 2001, and references therein]. These were intruded by 2690–2655 Ma high-Ca granites [*Champion and Sheraton*, 1997], though granite–greenstone contacts are commonly sheared. The maximum stratigraphic thickness of the greenstone succession is approximately 4–5 km [*Krapez et al.*, 2000], though significant structural repetition during regional pre-2670 Ma deformation has been recognized in the Kalgoorlie area [*Archibald et al.*, 1978; *Swager and Griffin*, 1990; *Blewett et al.*, 2004a]. However, it is unlikely that the regional thickness of the supracrustal complex exceeded 8 km when greenstone accumulation ceased at ca. 2665 Ma.

Dome-and-keel formation in the Goldfields at ca. 2650 Ma is widely attributed to regional WSW–ENE shortening,

which resulted in the exposure of granites as domal complexes in antiformal culminations [*Swager*, 1997; *Krapez et al.*, 2000]. *Blewett et al.* [2004a] attributed vertical amplification of the structures to relatively rapid switches in tectonic mode (coaxial horizontal shortening–extension–shortening over the interval 2670–2650 Ma). *Weinberg et al.* [2003] suggested that antiform nucleation was focused by pre-tectonic felsic plutons, with subsequent deformation at least partly attributable to solid-state, buoyancy-driven ascent of granites under conditions of slow compression.

THERMAL PARAMETERS

We now turn our attention to geophysical and geochemical data with the potential to constrain the syn-tectonic magnitudes of q_m, q_c, and z_c in the Pilbara and the Goldfields. The estimates obtained will be used (in combination with z_c–time evolutions synthesized from the relevant stratigraphic and geochronological data) in the next section, as input for thermal models simulating the greenstone accumulation history appropriate to each terrain, prior to dome-and-keel formation.

Archean q_c

Present-day surface heat flow (q_s) data provide important constraints on the magnitudes of q_c and q_m. Heat flow measurements in the Australian Archean are sparse [*Cull*, 1982], but typical q_s values are 40–50 mW m^{-2} in the Pilbara and 35–45 mW m^{-2} in the Goldfields [*Howard and Sass*, 1964; *Jaeger*, 1970; *Sass et al.*, 1976; *Cull and Denham*, 1979; *Cull*, 1991]. The overall tectonic quiescence of cratonic Western Australia during the Phanerozoic means that transient contributions to the measured surface heat flow are likely to be negligible, so equation (1) may be applied to the Archean terrains, in order to approximate q_s as the one-dimensional (vertical) sum of its independent components q_m and q_c. A first-order upper bound on present-day q_m is then obtained by using Fourier's Law:

$$q_m = k\frac{\Delta T_L}{\Delta z_L} \tag{8}$$

where ΔT_L is the temperature difference between the Earth's surface and the base of the conductive lithosphere, and Δz_L is the lithosphere thickness. Seismic tomography data suggest that the West Australian Archean lithosphere is 200–300 km thick [*Simons et al.*, 1999] and thermal modeling implies a depth of 170–230 km for the 1300 °C isotherm [*Artemieva and Mooney*, 2001]. Assuming Δz_L = 200–250 km, ΔT_L = 1280–1300 °C, and uniform thermal conductivity k = 3 W m^{-1} °C^{-1} for the lithosphere, equation (8) yields present-day q_m values in the range 15–20 mW m^{-2} for Western Australia. Such values are not significantly different from those obtained for a variety of Archean cratons worldwide [e.g., *Jones*, 1988; *Gupta et al.*, 1991; *Jaupart and Mareschal*, 1999; *Russell et al.*, 2001]. In fact, q_m must be lower than this, perhaps by as much as 5 mW m^{-2}, because of the contribution of heat production in the crust [e.g., *Jaupart and Mareschal,* 2003]. Of course, the present-day mantle heat flow has little bearing on the magnitude of the heat flow during Archean tectonism, which was likely to have been much higher (see later discussion).

By difference, equation (1) yields a lower bound (and therefore conservative) estimate for present-day q_c values of 20–35 mW m^{-2} for the Pilbara [*Bodorkos et al.*, 2004] and 15–30 mW m^{-2} for the Goldfields. Assuming these q_c values represent the respective present-day contributions of crust-hosted HPEs to the surface heat flux, we can calculate q_c values (corrected for the secular decline in radionuclide abundances) for each terrain at the time of Archean dome-and-keel formation. We used the present-day bulk-crustal element ratios K/U = 1.01 × 10^4 and Th/U = 3.9 [e.g., *McLennan and Taylor*, 1996] and obtained q_c ~ 50–90 mW m^{-2} for the Pilbara at 3300 Ma, and q_c ~ 30–60 mW m^{-2} for the Goldfields at 2650 Ma.

Initial (Pre-Greenstone) and Final (Post-Greenstone, Pre-Doming) Archean z_c Values

One-dimensional HPE depth distributions simulating greenstone-over-granite stratification were derived for each terrain by using two simple first-order assumptions. First, the Archean HPE content of the supracrustal greenstones is considered negligible. Second, we assume that the greenstone edifice overlies a geochemically undifferentiated felsic layer of unknown thickness, with an overall HPE budget dictated by its syn-tectonic q_c value and a uniform depth distribution of HPEs.

For the Pilbara, the geochemistry of this ancient felsic substrate was approximated directly by the 3490 Ma North Shaw granite suite, which has average K_2O = 2.5 wt%, Th = 11 ppm, and U = 2.5 ppm [*Bickle et al.*, 1989, 1993]. At a mean density ρ = 2800 kg m^{-3}, the volumetric heat production of this average composition was 4.10 μW m^{-3} at 3300 Ma. Our q_c estimate (50–90 mW m^{-2}) then corresponds to a North Shaw granitic layer thickness of approximately 12–22 km, prior to dome-and-keel formation at 3300 Ma. Unfortunately, analogous calculations in the Goldfields are complicated by the absence of felsic plutonic rocks that demonstrably predate accumulation of the greenstone succession. We therefore used the arithmetic mean of three geochemical averages from the highCa suite (K_2O = 2.9 wt%, Th = 12 ppm, and U = 3 ppm [*Champion and Sheraton*, 1997]), which is the oldest **[suite? oldest what?]** in the Goldfields, and accounts for over 60% of the granite Q2

exposure. For an average density $\rho = 2800$ kg m^{-3}, the volumetric heat production of the mean composition was 3.72 μW m^{-3} at 2650 Ma. Our q_c estimate (30–60 mW m^{-2}) then corresponds to a high-Ca granitic layer thickness of approximately 8–16 km, prior to dome-and-keel formation at 2650 Ma.

These layer-thickness data were then used to estimate the initial (pre-greenstone accumulation) and final (post-green-stone, pre-doming) characteristic depth of the heat production distribution (z_c) in each terrain [e.g., *Sandiford and Hand*, 1998; *Sandiford et al.*, 2002], which corresponds in each case to the depth midpoint of the HPE-bearing granitic layer (Figure 2). Initial z_c values for each terrain were obtained by simply halving the inferred thickness of the heat-producing layer (17 ± 5 km in the Pilbara, 12 ± 4 km in the Goldfields). Final z_c values were obtained by adding the initial z_c value to the pre-doming greenstone thickness (14 ± 3 km in the Pilbara, 6 ± 2 km in the Goldfields) in each case, yielding $z_c = 22.5 \pm 4$ km in the Pilbara at 3300 Ma and $z_c = 12 \pm 3$ km in the Goldfields at 2650 Ma [see also *Sandiford et al.*, 2004]. Equation (5) may then be used to estimate the *maximum* radiogenic contribution to the geotherm at and below the base of the heat-producing crust (i.e., T_c' at $z > z_2$; Figure 3), assuming that thermal equilibrium was attained in the interval separating the conclusion of green-tone accumulation and the initiation of dome-and-keel formation. The ranges of equilibrium T_c' values for the Goldfields (200 °C ± 100 °C) and the Pilbara (550 °C ± 250 °C) differ significantly, despite the partial overlap of the inferred q_c ranges (Figure 3), emphasizing the dependence of T_c' on z_c.

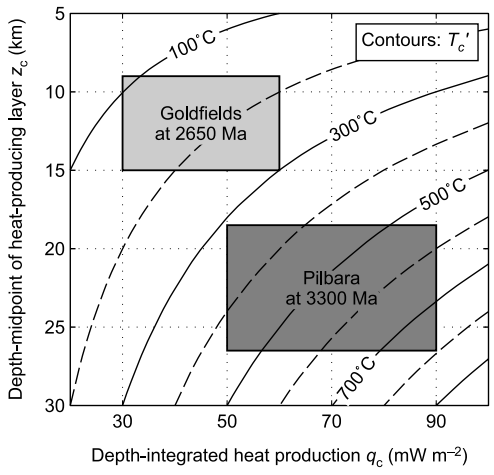

Figure 3. Diagram showing temperature at the base of the heat-producing crust with the ambient mantle component subtracted (T_c'), as a function of the abundance (q_c) and the depth distribution (z_c) of HPEs [see also *Sandiford and McLaren*, 2002]. The sensitivity of T_c' to z_c is highlighted by the large difference between the Pilbara ($T_c' = 300$–800 °C) and the Goldfields ($T_c' = 100$–300 °C) values, despite the partial overlap in their q_c ranges.

Archean q_m

It is widely believed that Archean mantle heat flow was significantly higher than the q_m values inferred for present-day Archean cratons, because the young Earth held more of its primordial heat [*McKenzie and Weiss*, 1975; *Thompson*, 1984; *Richter*, 1985; see also *Marshak*, 1999]. In addition, it is unlikely that the 200–300-km-thick lithospheric roots currently underlying almost all Archean cratons [e.g., *Artemieva and Mooney*, 2001] were present in their entirety during major tectono-magmatic activity in the overlying crust (although the thicknesses of such roots may have increased rapidly during the final stages of cratonization [e.g., *Pearson et al.*, 2002]). Secondly, geochemical data from Archean and modern mantle-derived mafic rocks suggest a decrease in primitive upper-mantle liquidus temperatures of the order of 150–200 °C since Mesoarchean times [e.g., *Abbott et al.*, 1994], and the results of parametrized mantle convection models imply a decrease in the mean mantle temperature of similar magnitude.

With respect to equation (8), these two considerations imply lower Δz_L and higher ΔT_L values, respectively, during the Archean, which act in concert to yield higher q_m values during active tectonism. Our simplified calculations assume a generalized Archean ΔT_L value of 1450 °C [*Abbott et al.*, 1994], and a syn-tectonic Δz_L value of 125 km, which is approximately half the seismic thickness of the lithospheric root currently underlying the Archean cratons of Western Australia. Combining these parameters with a time- and temperature-independent $k = 3$ W m^{-1} °C^{-1}, equation (8) yields an Archean q_m value of approximately 35 mW m^{-2}. We have adopted this q_m value for both terrains, for simplicity and in order to showcase the influence of q_c and z_c on the results of our thermal models.

THERMAL MODELING RESULTS

Now that we have derived Archean values for q_c, z_c and q_m in the Pilbara and the Goldfields, the thermal evolutions of crustal columns corresponding to the relevant greenstone deposition histories (prior to dome-and-keel formation) may be assessed. We solve the one-dimensional, time-dependent heat flow equation in a moving medium, which has the general form:

$$\rho c\left(\frac{\partial T}{\partial t} + U\frac{\partial T}{\partial z}\right) = k\frac{\partial^2 T}{\partial z^2} + H(z) \qquad (9)$$

where ρ is density, c is heat capacity, U is the vertical velocity (positive downward) of the reference frame (i.e., $U = \partial z/\partial t$), and $H(z)$ is the depth distribution of radiogenic heat production in the system. We adopted mid-range q_c

Table 1. Thermal Parameters and Geological Histories Modeled for the Pilbara and Goldfields[a].

Event/parameter	Pilbara	Goldfields
Initial configuration	3515 Ma	2715 Ma
Depth-integrated heat production (q_c)	70 mW m^{-2}	45 mW m^{-2}
Depth midpoint of uniform heat-producing layer (z_c)	8.5 km	6 km
First greenstone package		
Overall thickness (Δz_1)	8 km	6 km
Accumulation interval (Δt_1)	3515–3425 Ma	2715–2665 Ma
Time-averaged vertical velocity U_1 ($=\Delta z_1/\Delta t_1$)	89 m My^{-1}	120 m My^{-1}
New z_c ($=z_c + \Delta z_1$)	16.5 km at 3425 Ma	12 km at 2665 Ma
First period of quiescence ($U = 0$)	3425–3350 Ma (75 My)	2665–2650 Ma (15 My)
Second greenstone package		
Overall thickness (Δz_2)	6 km	–
Accumulation interval (Δt_2)	3350–3325 Ma	–
Time-averaged vertical velocity U_2 ($=\Delta z_2/\Delta t_2$)	240 m My^{-1}	–
New z_c ($=z_c + \Delta z_1 + \Delta z_2$)	22.5 km at 3325 Ma	–
Second period of quiescence ($U = 0$)	3325–3300 Ma (25 My)	–
Dome-and-keel formation	3300 Ma	2650 Ma

[a]The following time-invariant parameters are common to both models: $\rho = 3000$ kg m^{-3}, $c = 1$ kJ kg^{-1} °C^{-1}, $k = 3$ W m^{-1} °C^{-1}, $q_m = 35$ mW m^{-2}.

and z_c values for the initial configuration in each terrain (Table 1; see also Figure 3), and modeled the greenstone accumulation history by using the stratigraphic and geochronological data presented previously (Table 1). A basal boundary condition of constant heat flux ($q_m = 35$ mW m^{-2}) is applied throughout the modeled time, simply so we can clearly illustrate the thermal effects of changing heat production distribution.

Figure 4 shows the results in the form of a series of geotherms, corresponding to critical time-steps in each evolution. The results are most easily interpreted by considering the thermal evolution of the material point at the *base* of the heat-producing layer (indicated by a circle on each geotherm in Figure 4) in each model.

Goldfields

The initial (2715 Ma) temperature at the base of the 12-km-thick HPE-bearing layer in the Goldfields model was 230 °C, increasing to 350 °C (at a depth of 18 km) during the 2715–2665 Ma accumulation of the overlying 6 km-thick greenstone succession (Figure 4a). Nearly two-thirds of this temperature increase is due to the migration of the point down the mantle geotherm; he remainder is due to conductive incubation (i.e., steepening of the geotherm in response to the burial of HPEs). The heating rate is dictated by the thermal response time of the lithosphere, and in this case, significant thermal equilibration is achieved *during* greenstone accumulation, due to the relatively slow time-averaged burial rate (120 m My^{-1}; Table 1). Thermal equilibration and conductive incubation continued beyond the cessation of greenstone accumulation but were limited by the initiation of dome-and-keel formation at 2650 Ma, only 15 My after greenstone deposition was terminated. The conductive incubation-related temperature increase at 18 km depth over this period was only 20 °C (to $T = 370$ °C at 2650 Ma), representing approximately one-third of the temperature increase corresponding to complete thermal equilibration (depicted in Figure 4a by a theoretical 2550 Ma geotherm: $T = 405$ °C at 18 km depth after 115 My).

However, it is clear that conductive incubation in isolation will not result in significant heating within the greenstone-over-granite configuration corresponding to the Goldfields q_c, z_c, and q_m values, irrespective of equilibration time. Our model results suggest that at the time dome-and-keel formation was initiated at 2650 Ma, the effects of conductive incubation had not raised crustal temperatures ($z \leq 40$ km) above 600 °C, and that the HPE-bearing layer remained below the wet tonalite solidus throughout. Consequently, the 2650–2620 Ma granite magmatism observed in the Goldfields during and after dome-and-keel formation [e.g., *Smithies and Champion*, 1999] requires a significant additional source of heat.

Pilbara

The corresponding model for the Pilbara displays some important differences. Due to the combined effect of greater HPE abundances and a greater thickness, the initial temperature at the base of the heat-producing layer was significantly higher ($T = 396$ °C at 3515 Ma), and its increase during the first phase (3515–3425 Ma) of greenstone emplacement was much greater ($T = 588$ °C at 3425 Ma). This is partly due to

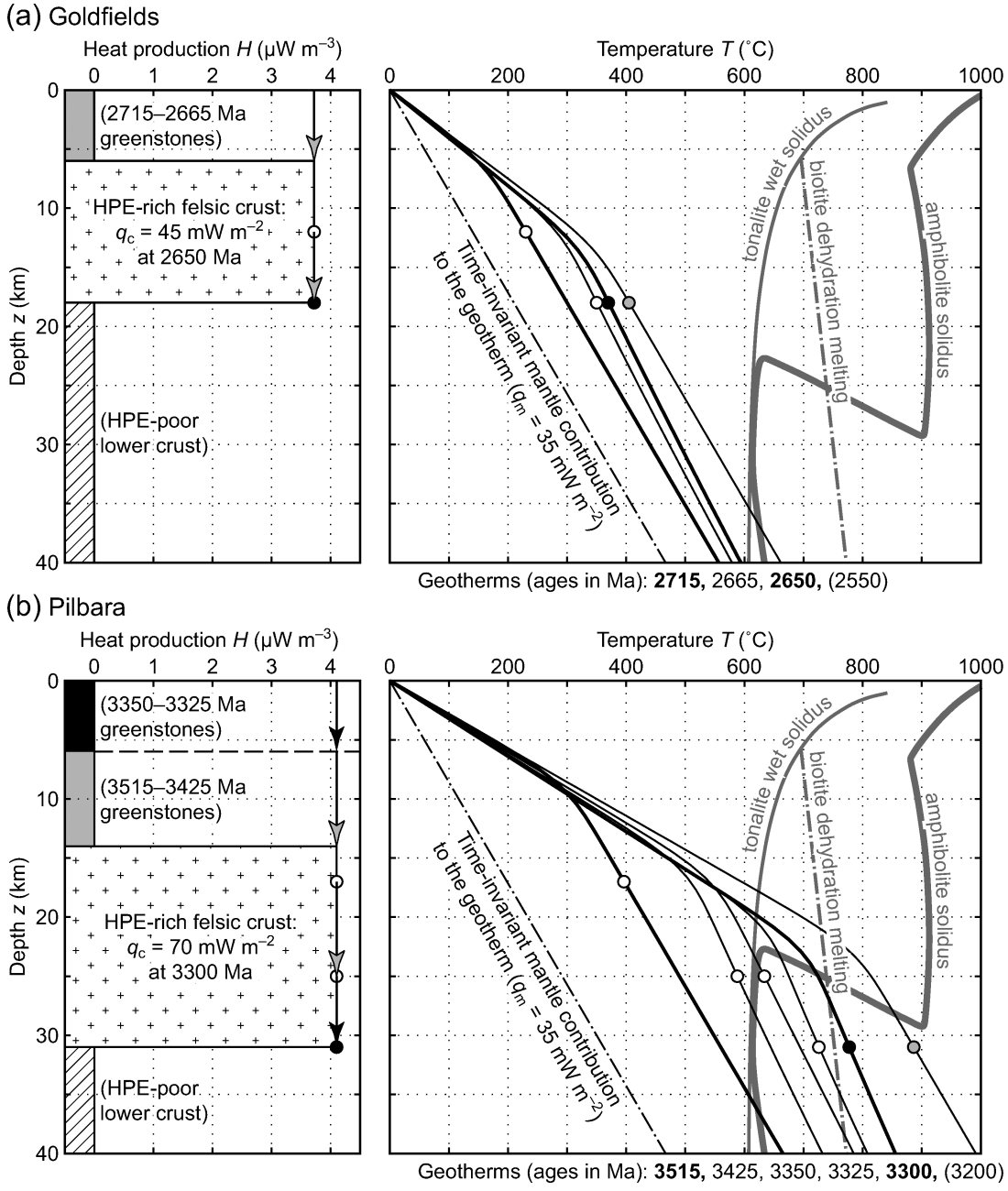

Figure 4. Input parameters and results of the one-dimensional thermal models for the Goldfields (a) and the Pilbara (b). In each case, the left panel shows the thickness and depth-independent heat production rate of the model TTG layer, with arrows showing the greenstone accumulation history (Table 1). The right panel shows the model results as a series of geotherms at critical times, with filled circles corresponding to the base of the HPE-bearing layer throughout. The heavy lines (with white and black circles, respectively) represent the initial and final (pre-doming) configurations; the gray circle represents a theoretical "final" geotherm, assuming thermal equilibrium was attained prior to dome-and-keel formation. The positions of the wet tonalite solidus, the amphibolite solidus, and the biotite dehydration melting reaction are those of *Zegers* [2004], following *Clemens and Wall* [1981], *Wolf and Wyllie* [1993], *Rapp* [1997], and *Wyllie et al.* [1997].

a greater greenstone thickness (8 km), but also because substantial syn-depositional thermal equilibration was permitted by the slow time-averaged accumulation rate (89 m My^{-1}; Table 1), similar to that observed in the Goldfields model. Conductive incubation further increased the temperature at 25 km depth to 634 °C over the 75-My period of quiescence from 3425 Ma until the second greenstone deposition event commenced at 3350 Ma.

During accumulation of the 6-km-thick 3350–3325 Ma greenstone succession, the temperature at the base of the heat-producing layer increased by 92 °C (to 726 °C at 31 km depth), mostly due to migration down the mantle geotherm, because the relatively rapid burial rate did not permit significant thermal equilibration. However, during the 25-My period of quiescence following the 3325 Ma cessation of greenstone accumulation, conductive incubation was responsible for a further temperature increase of 51 °C (to 777 °C at 31 km depth), prior to the initiation of dome-and-keel formation at 3300 Ma. The extent of this final heating episode is similar to the Goldfields model, in that it represents approximately one-third of the temperature increase corresponding to complete thermal equilibration (depicted in Figure 4b by a theoretical 3200 Ma geotherm: $T = 887$ °C at 31 km depth after 125 My).

Our model results suggest that for the combination of q_c, z_c, q_m, and greenstone accumulation history appropriate to the Pilbara prior to dome-and-keel formation, the base of the heat-producing layer probably lay on the high-temperature side of the wet solidi of tonalite and amphibolite and possibly also the fluid-absent biotite dehydration melting reaction (Figure 4b). This implies that conductive incubation *in isolation* was capable of generating granites via partial melting of pre-existing felsic crust and that such melting was broadly synchronous with dome-and-keel formation [e.g., *Sandiford et al.*, 2004]. The potential link between the two processes is considered in the following section.

THERMAL CONTROLS ON THE MECHANICAL BEHAVIOR OF THE CRUST

We now examine the influence of increasing mid-lower crustal temperature on the mechanical behavior of our greenstone-over-granite configurations, with emphasis on the role (and interplay) between two critical factors. First, the effective viscosities of crustal rocks are stress-dependent and decrease with increasing temperature [e.g., *Paterson*, 1987]. Second, the accumulation of thick greenstone successions atop HPE-rich felsic basement may result in a temperature increase sufficient to trigger partial melting (as illustrated in the previous section), and the presence of pseudo-Newtonian granitic magma in significant volumes may influence the rheology of the lower crust. Below, we outline the theoretical basis for our one-dimensional treatment of the effective (power-law) viscosity of the mid-crust as a function of temperature and melt fraction. This is followed by an assessment of the effect of **[inserted "of" ok?]**viscosity evolution at the base of the heat-producing layer in the Pilbara and the Goldfields. Q2

Relating Effective Viscosity to Temperature and Partial Melting

The influence of temperature on the effective viscosity of our greenstone-over-granite crust is considered in simplified fashion, by considering the buoyant ascent of a spherical, low-density felsic dome into an overlying, higher-density greenstone layer [e.g., *Weinberg and Podladchikov*, 1994]. Under natural physical conditions, most crustal rocks approximate power-law fluids, and in the case of uniaxial stress (σ), the equation

$$\dot{\varepsilon} = Ae^{-E/RT}\sigma^n \tag{10}$$

relates uniaxial strain rate ($\dot{\varepsilon}$), composition (where A, E, and n are material constants governing creep rates), and temperature (T), where R is the universal gas constant. The characteristic uniaxial stress is defined by

$$\sigma = \Delta\rho g r \tag{11}$$

where $\Delta\rho$ is the greenstone–granite density contrast, g is gravitational acceleration, and r is the dome radius. In this scenario, the effective viscosity (η_{eff}) is given by *Weinberg and Podladchikov* [1994] as follows:

$$\eta_{eff} = \frac{\sigma}{\dot{\varepsilon}} = \frac{e^{E/RT}}{A(\Delta\rho g r)^{n-1}} \tag{12}$$

We incorporated the influence of partial melting on effective viscosity by using a generalized model [following *Gerya and Yuen*, 2003] in which the melt fraction (M) within felsic crust at a specified pressure varies linearly over the temperature interval between the wet solidus (T_{wetsol}) and the dry liquidus (T_{dryliq}):

$$M = \frac{T - T_{wetsol}}{T_{dryliq} - T_{wetsol}} \tag{13}$$

This obviously represents a significant simplification, as most experimental data show nonlinear relationships between melt fraction and viscosity. The classical notion [e.g., *Arzi,* 1978; *van der Molen and Paterson,* 1979] that catastrophic loss of strength of a partially molten rock occurs at a critical melt fraction on the order of 0.3–0.5 (corresponding to breakdown of the solid framework) has recently been challenged by *Rosenberg and Handy* [2004], who contended that

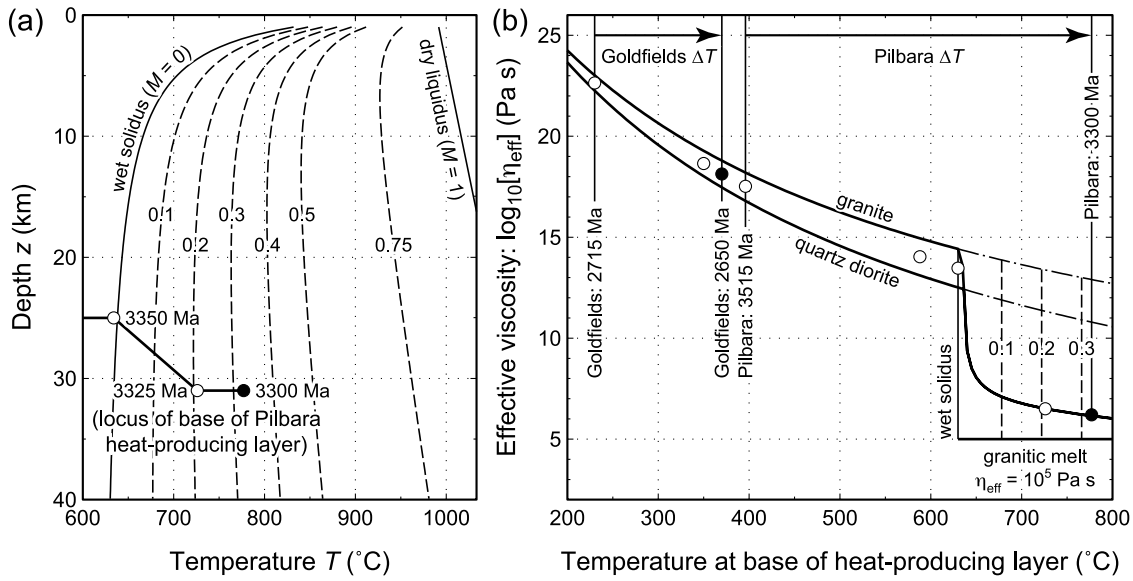

Figure 5. (a) Diagram summarizing the partial melting model used for felsic crust, following *Gerya and Yuen* [2003]. Melt fraction contours were constructed by using equation (13), and the *P–T* time path of the base of the Pilbara heat-producing layer is superimposed. (b) Diagram showing the temperature dependence of effective viscosity for a felsic dome with radius $r = 20$ km and density contrast $\Delta\rho = 250$ kg m^{-3} with respect to the overlying greenstones, over the temperature interval appropriate to the thermal evolutions modeled for the Pilbara and the Goldfields (circle fills are the same as Figure 4). The solid curves (at temperatures below the wet solidus) and their dot-dashed extensions (above the wet solidus) were constructed by using equation (12) and the following material parameters: "granite" $A = 2 \times 10^{-6}$ Mpa^{-n} s^{-1}, $E = 187$ kJ mol^{-1}, $n = 3.3$ [*Ji et al.*, 2003]; "quartz diorite" $A = 3 \times 10^{-2}$ Mpa^{-n} s^{-1}, $E = 212$ kJ mol^{-1}, $n = 2.4$ [*de Bremond d'Ars et al.*, 1999]. Above the wet solidus, the solid curve was constructed by using equations (13) and (14) with a temperature- and composition-independent η_{liq} value of 10^5 Pa s [e.g., *Clemens and Petford*, 1999]. The vertical dashed lines correspond to melt-fraction contours from (a).

the loss of strength corresponds to the onset of partial melting. Within the realm of low-volume partial melting appropriate to the thermal regimes considered in this study, our formulation corresponds most closely to the viscosity–melt fraction relationship proposed by *Rosenberg and Handy* [2004]. We used the pressure–temperature (*P–T*) loci for the wet solidus and dry liquidus (Figure 5a) fitted by *Gerya and Yuen* [2003] to the experimental data of *Johannes* [1985], *Schmidt and Poli* [1998], and *Poli and Schmidt* [2002], to estimate M as a function of temperature. The effective viscosity of the partially melted crust ($0 < M < 1$) was then estimated by using the equation derived by *Gay et al.* [1969] for high-concentration suspensions [see also *Pinkerton and Stevenson*, 1992]:

$$\eta_{eff} = \eta_{liq}\left\{\left[2.5 + \left(\frac{1-M}{M}\right)^{0.48}\right](1-M)\right\} \qquad (14)$$

where η_{liq} is the effective viscosity of granitic liquid. We assumed a uniform η_{liq} value of 10^5 Pa s to be representative of felsic liquids over the pressure, temperature, and water content ranges appropriate to the melting of TTG composition [see also *Scaillet et al.*, 1998; *Clemens and Petford*, 1999; *Holtz et al.*, 1999].

Crustal Mechanics in the West Australian Archean

We use the base of each heat-producing layer as a proxy for the Pilbara and Goldfield mid-crusts, which permits the effective viscosity evolutions directly corresponding to the thermal histories modeled in the previous section to be assessed. At subsolidus temperatures, equation (12) was used to estimate η_{eff}; in melt-bearing rocks, η_{eff} was approximated with equations (13) and (14). Figure 5b shows η_{eff} over the temperature interval spanning the Pilbara and Goldfields thermal histories for a felsic dome with radius $r = 20$ km, and density contrast $\Delta\rho = 250$ kg m^{-3} with respect to the overlying greenstones. The $\eta_{eff}(T)$ curves were constructed using equations (12) and (14), in combination with material parameters (A, E, and n) derived from the experimental data by **[insert "by" correct?]** *Hansen and Carter* [1982] for the end-members "granite" [*Ji et al.*, 2003] and "quartz diorite" [*de Bremond d'Ars et al.*, 1999]. Q2

No attempt has been made in either terrain to quantify the mechanical behavior of the upper crust in terms of its brittle yield strength. Consequently, the effective viscosity of the initial (2715 Ma) configuration in the Goldfields (from equation (12)) is very high ($\eta_{eff} = 10^{22}$–10^{23} Pa s; Figure 5b). Although it is likely that a power-law rheology is not appropriate at such low temperatures ($T = 230$ °C), the η_{eff} value obtained is a useful maximum against which to compare higher-T η_{eff} values. As documented in the previous section, the modeled 65-My history of burial and conductive incubation in the Goldfields produced a temperature increase $\Delta T = 140$ °C at the base of the heat-producing layer, corresponding to $\eta_{eff} \sim 10^{18}$ Pa s at 2650 Ma (Figure 5b). Conductive incubation may therefore have decreased the effective viscosity of the felsic layer by four to five orders of magnitude, prior to dome-and-keel formation. However, the low temperatures ($T < 400$ °C throughout; Figure 5b) precluded partial melting of the felsic substrate in the absence of a substantial external heat source. It is thus unlikely that burial and conductive incubation in isolation had the capacity to modify the rheological behavior of the Goldfields crust to the point where purely buoyancy-driven dome-and-keel formation was a viable process.

The contrast between the Goldfields and Pilbara models is best illustrated by the similarity between the *final* (2650 Ma) configuration of the former (prior to dome-and-keel formation) and the *initial* (3515 Ma) condition of the latter, in terms of temperature (and therefore η_{eff}) at the base of the felsic crust. For the same range of A, E, and n values, Pilbara η_{eff} values decreased by approximately four orders of magnitude (from 5×10^{17} Pa s at 3515 Ma to 5×10^{13} Pa s at 3350 Ma) *prior* to the initiation of partial melting (Figure 5). Once melt production commenced (at $T \sim 635$ °C; Figure 5a), η_{eff} declined sharply with increasing M (Figure 5b), until the effective viscosity of the crystal–melt suspension at the base of the heat-producing layer resembled that of a granitic liquid, prior to dome-and-keel formation ($\eta_{eff} \sim 10^6$ Pa s for $M > 0.3$ at 3300 Ma; Figure 5b). Although our $\eta_{eff}(T)$–M model neglects the obvious possibility of progressive, batch-wise melt removal [e.g., *Sawyer*, 1994; *Rutter*, 1997; *Bons et al.*, 2004] and the potential for associated "stiffening" of the residual heat-producing layer, it is very likely that the modeled thermal history resulted in a substantially decreased effective viscosity in the Pilbara mid-crust. Dome-and-keel formation may have been initiated by large-scale, buoyancy-driven ascent of the crystal–melt suspension, triggering partial convective overturn of the crust [*Collins et al.*, 1998; *Van Kranendonk et al.*, 2002] that was assisted and sustained by the gravitational instability imposed by the overlying 11–17-km-thick greenstone edifice.

IMPLICATIONS FOR THE EVOLUTION OF ARCHEAN DEFORMATION STYLE

Our model results highlight the relative inefficiency of conductive incubation as a mechanism for raising upper- to mid-crustal temperatures in the Goldfields at the time of 2650 Ma dome-and-keel formation. This is primarily due to low HPE abundances in the felsic basement ($q_c = 45 \pm 15$ mW m^{-2}), and the relatively short period (65 My) over which the relatively thin (6–10-km-thick) greenstone edifice accumulated. Consequently, temperatures remained below 400 °C throughout, and it is unlikely that the effective viscosity of the mid-crust was significantly affected by conductive incubation (Figure 5b). We therefore contend that the link between the deformation history preserved by macroscopic structures and the physical processes governing deformation is similar to that characteristic of post-Archean tectonism at terrain-scale: Most large-scale structures developed in direct response to large, horizontally directed body forces and were "locked in" by a mechanically strong upper- to mid-crust. Dome-and-keel structure in the Goldfields (Figure 1) is characterized by the preservation of broad, granite-cored D2 antiforms in preference to the intervening greenstone-dominated synforms [*Blewett et al.*, 2004a], which may reflect antiform nucleation controlled by buoyancy-driven ascent of the underlying granites in the solid state [*Weinberg et al.*, 2003].

The Pilbara model results represent a stark contrast, because the heat production rate of the Pilbara felsic basement was 50–100% higher ($q_c = 70 \pm 20$ mW m^{-2}), the greenstone carapace was 50–100% thicker (11–17 km), and the duration of accumulation and thermal equilibration (215 My) was 200% longer. As a result, initial temperatures of approximately 400 °C at the base of the Pilbara heat-producing layer were elevated to 750–800 °C by conductive incubation, potentially reducing the effective viscosity of the mid-crust by several orders of magnitude (Figure 5). Thermal and mechanical softening was exacerbated by partial melting of the mid- to lower-crustal felsic layer and was amplified by the inherent large-scale density inversion. This resulted in a patently unstable crustal configuration (characterized by high q_c and z_c values) for which there is no equivalent in the modern Earth.

This thermo-mechanical instability had two potentially important implications. First, in terms of buoyancy and gravitational effects, the internal instability of the reverse-stratified system rendered it susceptible to large-scale deformation by external body forces that need not have been large in comparison with those acting along the boundaries of converging plates in the modern Earth. Second, and equally importantly, the rock record of such a perturbation event may be obscured, or even obliterated, by subsequent large-scale

deformation associated with the attainment of a more stable configuration.

In this context, the crustal scale at which "classical" dome-and-keel structure developed is important, because low mid-crustal effective viscosities in isolation are unlikely to trigger large-scale dome-and-keel formation without significant weakening and/or brittle rupture of the overlying greenstone-dominated upper crust at similar scale [e.g., *Bleeker*, 2002]. Early extension in the upper crust may therefore be critical to the successful development of dome-and-keel structure [e.g., *Martinez et al.*, 2001; *Bleeker*, 2002], but the record of such a process may be poorly preserved and/or difficult to recognize within a deformation framework dominated by large-scale partial convective overturn of the crust. Consequently, fundamental differences may exist between the hot, soft syn-tectonic crust typical of the Pilbara (and possibly other Mesoarchean granite–greenstone terrains featuring classical dome-and-keel architecture; *Choukroune et al.* [1995]) and the colder, stronger crust typical of younger terrains, with respect to the relationship(s) between the physical processes governing deformation and the structures developed and preserved.

Such thermal-mechanical feedbacks are likely to have important implications for crustal behavior and tectonic style in Archean granite–greenstone terrains. In thermal terms, large-scale diapiric ascent of granitic magmas derived from ancient felsic basement represented an extremely efficient mechanism for reconcentrating HPEs in the upper crust [*Sandiford et al.*, 2002; 2004]. In the Pilbara, the resulting re-establishment of a configuration comparable to the initial condition via granite doming inevitably led to significant long-term cooling (and therefore strengthening) of the lower crust. It is thus possible that the physical conditions prevailing during Archean crustal construction were not merely favorable with respect to dome-and-keel formation, but that such vertical reorganization of the crust was *necessary* (together with rapid development of thick lithospheric mantle roots; e.g., *Pollack* [1986]; *Pearson et al.* [2002]) for the preservation of HPE-rich crustal segments at craton-scale, without significant reworking [e.g,, *Morgan*, 1985].

CONCLUSIONS

Conductive incubation is an important source of "internal" heat in Archean granite–greenstone terrains. In this study we have illustrated the sensitivity of mid-crustal temperature (and, by association, effective viscosity) to the first-order geological and tectono-stratigraphic features of the contrasting Pilbara and Goldfields terrains in Western Australia. Our one-dimensional thermal modeling of greenstone-over-granite crustal evolution has highlighted a large temperature difference at the base of the heat-producing layer in each terrain, prior to dome-and-keel formation ($T = 370$ °C at 18 km depth in the Goldfields at 2650 Ma; $T = 777$ °C at 31 km depth in the Pilbara at 3300 Ma). This contrast primarily reflects the concerted influence of interterrain differences in the syn-tectonic crustal HPE budget (q_c), the thicknesses of the greenstone successions accumulated atop ancient felsic basement (z_c), and the timescales over which greenstone accumulation took place.

The prevalence of low temperatures (and relatively small temperature increases) in the Goldfields model implies a dominantly brittle upper-mid-crust rheology and probably precludes a significant role for conductive incubation in isolation with respect to reducing the effective viscosity of the Goldfields crust ($\eta_{eff} = 10^{18}$–10^{23} Pa s throughout). In contrast, higher initial temperatures (and much larger temperature increases) at the base of the heat-producing layer in the Pilbara model resulted in significant effective viscosity decreases, from $\eta_{eff} = 5 \times 10^{17}$ Pa s at 3515 Ma to $\eta_{eff} < 10^{10}$ Pa s prior to dome-and-keel formation at 3300 Ma. These low effective viscosities were largely due to in situ partial melting of the felsic crust during conductive incubation which, in combination with the density inversion inherent in the greenstone-over-granite configuration, uniquely favored large-scale, classical dome-and-keel formation in the Pilbara.

The differing crustal rheologies produced by the contrasting Pilbara and Goldfields thermal regimes may reflect secular differences between Mesoarchean and younger terrains, with respect to the physical processes responsible for first-order structural development of the Archean crust. This study advocates the development of classical dome-and-keel structure in the Pilbara as a predominantly thermal response to substantial greenstone accumulation, driven "internally" by the imperative of attaining (via large-scale reconcentration of HPEs in the upper crust) a thermo-mechanically sustainable configuration [e.g., *Sandiford et al.*, 2004]. This does not preclude the possibility that dome-and-keel formation was triggered or assisted by a horizontally directed "external" tectonic force (significant or otherwise), but the structural record of such an event may be difficult to recognize due to the pervasive structural overprinting associated with subsequent vertical reorganization of the crust.

In contrast, the rheology of the Goldfields crust was probably not significantly affected by conductive incubation, so the greenstone-over-granite configuration had greater intrinsic stability. Dome-and-keel formation was therefore probably driven by external horizontally directed plate tectonic forces [e.g., *Blewett et al.*, 2004a], with the shallowing of HPEs associated with granite ascent playing only a supporting role in stabilizing the crust. This colder, stronger crust is correspondingly more likely to lock in a direct record of such far-field forcing, analogous to the record typically preserved in modern orogenic belts.

Acknowledgments. We thank Roberto Weinberg for stimulating and informative discussions that refined these ideas, and Jean-Claude Mareschal, Olivier Vanderhaeghe, and an anonymous reviewer for formal reviews that resulted in important clarifications to an earlier version of the manuscript. The Australian Research Council supported this research, via grants DP0208176 (awarded to S. Bodorkos) and DP0209157 and F10020050 (awarded to M. Sandiford).

REFERENCES

Abbott, D., L. Burgess, J. Longhi, and W.H.F. Smith (1994), An empirical thermal history of the Earth's upper mantle, *J. Geophys. Res.*, 99, 13835-13850.

Anhaeusser, C.R., R. Mason, M.J. Viljoen, and R.P. Viljoen (1969), A reappraisal of some aspects of Precambrian shield geology, *Geol. Soc. Am. Bull.*, 80, 2175-2200.

Archibald, N.J., L.F. Bettenay, R.A. Binns, D.I. Groves, and R.J. Gunthorpe (1978), The evolution of Archaean granite-greenstone terrains, Eastern Goldfields Province, Western Australia, *Precambrian Res.*, 6, 103-131.

Artemieva, I.M., and W.D. Mooney (2001), Thermal thickness and evolution of Precambrian lithosphere: a global study, *J. Geophys. Res.*, 106, 16387-16414.

Arzi, A.A. (1978), Critical phenomena in the rheology of partially melted rocks. *Tectonophysics*, 44, 173-184.

Bagas, L., M.J. Van Kranendonk, and M. Pawley (2004), Geology of the Split Rock 1:100 000 sheet, Western Australia, *1:100 000 Geological Series Explanatory Notes*, 43 pp., Geol. Surv. West. Aust., Perth.

Barley, M.E., and A.L. Pickard (1999), An extensive, crustally-derived, 3325 to 3310 Ma silicic volcanoplutonic suite in the eastern Pilbara Craton: evidence from the Kelly Belt, McPhee Dome, and Corunna Downs Batholith, *Precambrian Res.*, 96, 41-62.

Bickle, M.J., L.F. Bettenay, H.J. Chapman, D.I. Groves, N.J. McNaughton, I.H. Campbell, and J.R. de Laeter (1989), The age and origin of younger granitic plutons of the Shaw Batholith in the Archaean Pilbara Block, Western Australia, *Contrib. Mineral. Petrol.*, 101, 361-376.

Bickle, M.J., L.F. Bettenay, H.J. Chapman, D.I. Groves, N.J. McNaughton, I.H. Campbell, and J.R. de Laeter (1993), Origin of the 3500–3300 Ma calc-alkaline rocks in the Pilbara Archaean: isotopic and geochemical constraints from the Shaw Batholith, *Precambrian Res.*, 60, 117-149.

Bleeker, W. (2002), Archaean tectonics: a review, with illustrations from the Slave Craton, in *The Early Earth: Physical, Chemical and Biological Development*, edited by C.M.R. Fowler, C.J. Ebinger, and C.J. Hawkesworth, *Geol. Soc. London Spec. Publ.* 199, pp. 151-181.

Blewett, R.S. (2002), Archaean tectonic processes: a case for horizontal shortening in the North Pilbara Granite-Greenstone Terrane, Western Australia, *Precambrian Res.*, 113, 87-120.

Blewett, R.S., K.F. Cassidy, D.C. Champion, P.A. Henson, B.S. Goleby, L. Jones, and P.B. Groenewald (2004a), The Wangkathaa Orogeny: an example of episodic regional 'D_2' in the late Archaean Eastern Goldfields Province, Western Australia, *Precambrian Res.*, 130, 139-159.

Blewett, R.S., S. Shevchenko, and B. Bell (2004b), The North Pole Dome: a non-diapiric dome in the Archaean Pilbara Craton, Western Australia, *Precambrian Res.*, 133, 105-120.

Bodorkos, S., M. Sandiford, B.R.S. Minty, and R.S. Blewett (2004), A high-resolution, calibrated airborne radiometric dataset applied to the estimation of crustal heat production in the Archaean northern Pilbara Craton, Western Australia, *Precambrian Res.*, *128*, 57-82.

Bons, P.D., J. Arnold, M.A. Elburg, J. Kalda, A. Soesoo, and B. van Milligen (2004), Melt extraction and accumulation from partially molten rocks, *Lithos*, 78, 25-42.

Brown, S.J.A., B. Krapez, S.W. Beresford, K.F. Cassidy, D.C. Champion, M.E. Barley, and R.A.F. Cas (2001), Archaean volcanic and sedimentary environments of the Eastern Goldfields province, Western Australia – a field guide, *Geol. Surv. West. Aust. Record*, 2001/13, 66 pp.

Buick, R., J.R. Thornett, N.J. McNaughton, J.B. Smith, M.E. Barley, and M. Savage (1995), Record of emergent continental crust ~3.5 billion years ago in the Pilbara craton of Australia, *Nature*, 375, 574-577.

Card, K.D. (1990), A review of the Superior Province of the Canadian Shield: a product of Archaean accretion, *Precambrian Res.*, 48, 99-156.

Champion, D. C., and J. W. Sheraton (1997), Geochemistry and Nd isotope systematics of Archaean granites of the Eastern Goldfields, Yilgarn Craton, Australia: implications for crustal growth processes, *Precambrian Res.*, 83, 109-132.

Chardon, D., P. Choukroune, and M. Jayananda (1996), Strain patterns, dÈcollement and incipient sagducted greenstone terrains in the Archaean Dharwar craton (south India), *J. Struct. Geol.*, 18, 991-1004.

Chardon, D., P. Choukroune, and M. Jayananda (1998), Sinking of the Dharwar Basin (South India): implications for Archaean tectonics, *Precambrian Res.*, 91, 15-39.

Chardon, D., J.J. Peucat, M. Jayananda, P. Choukroune, and C.M. Fanning (2002), Archean granite-greenstone tectonics at Kolar (South India): Interplay of diapirism and bulk inhomogeneous contraction during juvenile magmatic accretion, *Tectonics*, 21(3), DOI: 10.1029/2001TC901032.

Choukroune, P., H. Bouhallier, and N.T. Arndt (1995), Soft lithosphere during periods of Archaean crustal growth or crustal reworking, in *Early Precambrian Processes*, edited by M.P. Coward and A. C. Ries, *Geol. Soc. London Spec. Publ.*, 95, pp. 67-86.

Choukroune, P., J.N. Ludden, D. Chardon, A.J. Calvert, and H. Bouhallier (1997), Archaean crustal growth and tectonic processes: a comparison of the Superior Province, Canada and the Dharwar Craton, India, in *Orogeny Through Time*, edited by J.-P. Burg and M. Ford, *Geol. Soc. London Spec. Publ.*, 121, pp. 63-98.

Clemens, J.D., and N. Petford (1999), Granitic melt viscosity and silicic magma dynamics in contrasting tectonic settings, *J. Geol. Soc. London*, 156, 1057-1060.

Clemens, J.D., and V.J. Wall (1981), Origin and crystallization of some peraluminous (S-type) granitic magmas, *Can. Mineral.*, 19, 111-131.

Collins, W.J. (1989), Polydiapirism of the Archean Mount Edgar Batholith, Pilbara Block, Western Australia, *Precambrian Res.*, 43, 41-62.

Collins, W.J., M.J. Van Kranendonk, and C. Teyssier (1998), Partial convective overturn of Archaean crust in the east Pilbara Craton, Western Australia: driving mechanisms and tectonic implications, *J. Struct. Geol.*, 20, 1405-1424.

Cull, J.P. (1982), An appraisal of Australian heat-flow data, *BMR J. Aust. Geol. Geophys.*, 7, 11-21.

Cull, J.P. (1991), Heat flow and regional geophysics in Australia, in *Terrestrial Heat Flow and the Lithosphere Structure*, edited by V. Cermak and L. Rybach, pp. 486–500, Springer-Verlag, Berlin.

Cull, J.P., and D. Denham (1979), Regional variations in Australian heat flow, *BMR J. Aust. Geol. Geophys.*, 4, 1-13.

de Bremond d'Ars, J., C. Lécuyer, and B. Reynard (1999), Hydrothermalism and diapirism in the Archean: gravitational instability constraints, *Tectonophysics*, 304, 29-39.

de Wit, M.J. (1998), On Archean granites, greenstones, cratons and tectonics: does the evidence demand a verdict?, *Precambrian Res.*, 91, 181-226.

de Wit, M.J., and L.D. Ashwal (1997), Greenstone Belts, Oxford University Press, Oxford.

Gay, E.C., P.A. Nelson, and W.P. Armstrong (1969), Flow properties of suspensions with high solids concentrations, *Am. Inst. Chem. Eng. J.*, 15, 815-822.

Gerya, T.M., and D.A. Yuen (2003), Rayleigh-Taylor instabilities from hydration and melting propel 'cold plumes' at subduction zones, *Earth Planet. Sci. Lett.*, 212, 47-62.

Goleby, B.R., R.S. Blewett, R.J. Korsch, D.C. Champion, K.F. Cassidy, L.E.A. Jones, P.B. Groenewald, and P.A. Henson (2004), Deep seismic reflection profiling in the Archaean northeastern Yilgarn Craton, Western Australia: implications for crustal architecture and mineral potential, *Tectonophysics*, 388, 119-133.

Green, M.G., P.J. Sylvester, and R. Buick (2000), Growth and recycling of early Archaean continental crust: geochemical evidence from the Coonterunah and Warrawoona Groups, Pilbara Craton, Australia, *Tectonophysics*, 322, 69-88.

Griffin, T.J. (1990), Eastern Goldfields Province, in *Geology and Mineral Resources of Western Australia*, *Geol. Surv. West. Aust. Memoir*, 3, pp. 77-119.

Gupta, M.L., A. Sundar, and S.R. Sharma (1991), Heat flow and heat generation in the Archaean Dharwar cratons and implications for the southern Indian Shield geotherm and lithospheric thickness, *Tectonophysics*, 194, 107-122.

Hamilton, W.B. (1998), Archaean magmatism and deformation were not products of plate tectonics, *Precambrian Res.*, 91, 143-179.

Hansen, F.D., and N.L. Carter (1982), Creep of selected crustal rocks at 1000 MPa, *EOS Trans. AGU*, 63, 437.

Henry, P., R.K. Stevenson, Y. Larbi, and C. Gariepy (2000), Nd isotopic evidence for Early to Late Archaean (3.4–2.7 Ga) crustal growth in the Western Superior Province (Ontario, Canada), *Tectonophysics*, 322, 135-151.

Hickman, A.H. (1983), Geology of the Pilbara Block and its environs, *Geol. Surv. West. Aust. Bulletin*, 127, 268 pp.

Hickman, A.H. (1984), Archaean diapirism in the Pilbara Block, Western Australia, in *Precambrian Tectonics Illustrated*, edited by A. Köner, and R. Greiling, pp. 113-127, E. Schweizerbart'sche Verlagsbuch-handlung, Stuttgart.

Hickman, A.H., and M.J. Van Kranendonk (2004), Diapiric processes in the formation of Archaean continental crust, East Pilbara Granite-Greenstone Terrane, Australia, in *The Precambrian Earth: Tempos and Events*, edited by P.G. Eriksson, W. Altermann, D.R. Nelson, W.U. Mueller, and O. Catuneanu, pp. 118-139, Elsevier, Amsterdam.

Holtz, F., J. Roux, S. Ohlhorst, H. Behrens, and F. Schulze (1999), The effects of silica and water on the viscosity of hydrous quartzofeldspathic melts, *Am. Mineral.*, 84, 27-36.

Howard, L.E., and J.H. Sass (1964), Terrestrial heat flow in Australia, *J. Geophys. Res.*, 69, 1617-1626.

Jaeger, J.C. (1970), Heat flow and radioactivity in Australia, *Earth Planet. Sci. Lett.*, 8, 285–292.

Jaupart, C., and J.C. Mareschal (1999), The thermal structure and thickness of continental roots, *Lithos*, 48, 93-114.

Jaupart, C., and J.C. Mareschal (2003), Constraints on crustal heat production from heat flow data, in *Treatise on Geochemistry: Volume 3: The Crust*, edited by R.L. Rudnick, pp. 65-84, Elsevier Pergamon, Oxford.

Jelsma, H.A., P.A. van der Beek, and M.L. Vinyu (1993), Tectonic evolution of the Bindura-Shamva greenstone belt (northern Zimbabwe) – progressive deformation around diapiric batholiths, *J. Struct. Geol.*, 15, 163-176.

Ji, S., P. Zhao, and B. Xia (2003), Flow laws of multiphase materials and rocks from end-member flow laws, *Tectonophysics*, 370, 129-145.

Johannes, W. (1985), The significance of experimental studies for the formation of migmatites, in *Migmatites*, edited by J.R. Ashworth, pp. 36-85, Blackie, Glasgow.

Jones, M.Q.W. (1988), Heat flow in the Witwatersrand Basin and environs and its significance for the South African shield geotherm and lithospheric thickness, *J. Geophys. Res.*, 93, 3243-3260.

Kloppenburg, A., S.H. White, and T.E. Zegers (2001), Structural evolution of the Warrawoona Greenstone Belt and adjoining granitoid complexes, Pilbara Craton, Australia: implications for Archaean tectonic processes, *Precambrian Res.*, 112, 107-147.

Krapez, B., S.J.A. Brown, J. Hand, M.E. Barley, and R.A.F. Cas (2000), Age constraints on recycled crustal and supracrustal sources of Archaean metasedimentary sequences, Eastern Goldfields Province, Western Australia: evidence from SHRIMP zircon dating, *Tectonophysics*, 322, 89-133.

Macgregor, A.M. (1951), Some milestones in the Precambrian of southern Rhodesia, *Proc. Geol. Soc. S. Afr.*, 54, 27-71.

Mareschal, J.-C., and G.F. West (1980), A model for Archean tectonism. Part 2. Numerical models of vertical tectonism in greenstone belts, *Can. J. Earth Sci.*, 17, 60-71.

Marshak, S. (1999), Deformation style way back when: thoughts on the contrast between Archean/Palaeoproterozoic and contemporary orogens, *J. Struct. Geol.*, 21, 1175-1182.

Marshak, S., F.F. Alkmim, and H. Jordt-Evangelista (1992), Proterozoic crustal extension and the generation of dome-and-keel structure in an Archean granite-greenstone terrane, *Nature*, 357, 491-493.

Martinez, F., A.M. Goodliffe, and B. Taylor (2001), Metamorphic core complex formation by density inversion, *Nature*, 411, 930-934.

McKenzie, D., and N. Weiss (1975), Speculations on the thermal and tectonic history of the Earth, *Geophys. J. R. Astronom. Soc.*, 42, 131-174.

McLennan, S.M., and S.R. Taylor (1996), Heat flow and the chemical composition of continental crust, *J. Geol.*, 104, 369-377.

Morgan, P. (1985), Crustal radiogenic heat production and the selective survival of ancient continental crust, *J. Geophys. Res.*, 90, C561-C570.

Myers, J.S. (1997), Preface: Archaean geology of the Eastern Goldfields of Western Australia – regional overview, *Precambrian Res.*, 83, 1-10.

Myers, J.S., R.D. Shaw, and I.M. Tyler (1996), Tectonic evolution of Proterozoic Australia, *Tectonics*, 15, 1431-1446.

Nelson, D.R. (1997), Evolution of the Archaean granite-greenstone terranes of the Eastern Goldfields, Western Australia: SHRIMP U-Pb constraints, *Precambrian Res.*, 83, 57-81.

Paterson, M.S. (1987), Problems in the extrapolation of laboratory rheological data, *Tectonophysics*, 133, 33-43.

Pearson, D.G., G.J. Irvine, R.W. Carlson, M.G. Kopylova, and D.A. Ionov (2002), The development of lithospheric keels beneath the earliest continents: time constraints using PGE and Re–Os isotope systematics, in *The Early Earth: Physical, Chemical and Biological Development*, edited by C.M.R. Fowler, C.J. Ebinger, and C. J. Hawkesworth, *Geol. Soc. London Spec. Publ.*, 199, pp. 65-90.

Percival, J.A., V. McNicoll, J.L. Brown, and J.B. Whalen (2004), Convergent margin tectonics, central Wabigoon subprovince, Superior Province, Canada, *Precambrian Res.*, 132, 213-244.

Peschler, A.B., K. Benn, and W.R. Roest (2004), Insights on Archean continental dynamics from gravity modelling of granite greenstone terranes, *J. Geodyn.*, 38, 185-207.

Pinkerton, H., and R.J. Stevenson (1992), Methods of determining the rheological properties of magmas at sub-liquidus temperatures, *J. Volcanol. Geotherm. Res.*, 53, 47-66.

Poli, S., and M.W. Schmidt (2002), Petrology of subducted slabs, *Ann. Rev. Earth Planet. Sci.*, 30, 207-235.

Pollack, H.N. (1986), Cratonization and thermal evolution of the mantle, *Earth Planet. Sci. Lett.*, 80, 175-182.

Pollack, H.N. (1997), Thermal characteristics of the Archaean, in *Greenstone Belts*, edited by M.J. de Wit and L.D. Ashwal, pp. 223-232, Clarendon Press, Oxford.

Pysklywec, R.N., and C. Beaumont (2004), Intraplate tectonics: feedback between radioactive thermal weakening and crustal deformation driven by mantle lithosphere instabilities, *Earth Planet. Sci. Lett.*, 221, 275-292.

Rapp, R.P. (1997), Heterogeneous source regions for Archaean granitoids: experimental and geochemical evidence, in *Greenstone Belts*, edited by M.J. de Wit and L.D. Ashwal, pp. 267-279, Clarendon Press, Oxford.

Richter, F.M. (1985), Models for the Archean thermal regime, *Earth Planet. Sci. Lett.*, 73, 350-360.

Ridley, J.R., and J.D. Kramers (1990), The evolution and tectonic consequences of a tonalitic magma layer within Archean continents, *Can. J. Earth Sci.*, 27, 219-228.

Rosenberg, C.L., and M.R. Handy (2004), Experimental deformation of partially melted granite revisited: implications for the continental crust, *J. Metamorph. Geol.*, 23, 19-28.

Russell, J.K., G.M. Dipple, and M.G. Kopylova (2001), Heat production and heat flow in the mantle lithosphere, Slave craton, Canada, *Phys. Earth Planet. Interiors*, 123, 27-44.

Rutter, E.H. (1997), The influence of deformation on the extraction of crustal melts: a consideration of the role of melt-assisted granular flow, in *Deformation-Enhanced Fluid Transport in the Earth's Crust and Mantle*, edited by M.B. Holness, pp. 82-110, Chapman and Hall, London.

Sandiford, M., and M. Hand (1998), Australian Proterozoic high-temperature, low-pressure metamorphism in the conductive limit, in *What Drives Metamorphism and Metamorphic Reactions?*, edited by P. J. Treloar and P.J. O'Brien, *Geol. Soc. London Spec. Publ.*, 138, pp. 109-120.

Sandiford, M., and S. McLaren (2002), Tectonic feedback and the ordering of heat producing elements within the continental lithosphere, *Earth Planet. Sci. Lett.*, 204, 133-150.

Sandiford, M., S. McLaren, and N. Neumann (2002), Long-term thermal consequences of the redistribution of heat-producing elements associated with large-scale granitic complexes, *J. Metamorph. Geol.*, 20, 87-98.

Sandiford, M., M.J. Van Kranendonk, and S. Bodorkos (2004), Conductive incubation and the origin of dome-and-keel structure in Archaean granite-greenstone terrains: a model based on the eastern Pilbara Craton, Western Australia, *Tectonics*, 23, TC1009, DOI: 10.1029/2002TC001452.

Sass, J.H., J.C. Jaeger, and R.J. Munroe (1976), Heat flow and near surface radioactivity in the Australian continental crust, *U.S. Geol. Surv., Open File Report*, 76-250.

Sawyer, E.W. (1994), Melt segregation in the continental crust, *Geology*, 22, 1019-1022.

Scaillet, B., F. Holtz, and M. Pichavant (1998), Phase equilibrium constraints on the viscosity of silicic magmas–1. Volcano-plutonic association, *J. Geophys. Res.*, 103, 27257-27266.

Schmidt, M.W., and S. Poli (1998), Experimentally based water budgets for dehydrating slabs and consequences for arc magma generation, *Earth Planet. Sci. Lett.*, 163, 361-379.

Simons, F.J., A. Zielhuis, and R.D. van der Hilst (1999), The deep structure of the Australian continent from surface wave tomography, *Lithos*, 48, 17-43.

Smithies, R.H., and D.C. Champion (1999), Late Archaean felsic alkaline igneous rocks in the Eastern Goldfields, Yilgarn Craton, Western Australia: a result of lower crustal delamination?, *J. Geol. Soc. London*, 156, 561-576.

Smithies, R.H., D.C. Champion, and K.F. Cassidy (2003), Formation of Earth's early Archaean continental crust, *Precambrian Res.*, 127, 89-101.

Swager, C.P. (1997), Tectono-stratigraphy of late Archaean greenstone terranes in the southern Eastern Goldfields, Western Australia, *Precambrian Res.*, 83, 11-42.

Swager, C.P., B.R. Goleby, B.J. Drummond, M.S. Rattenbury, and P.R. Williams (1997), Crustal structure of granite-greenstone terranes in the Eastern Goldfields, Yilgarn Craton, as revealed by seismic reflection profiling, *Precambrian Res.*, 83, 43-56.

Swager, C.P., and T.J. Griffin (1990), An early thrust duplex in the Kalgoorlie-Kambalda greenstone belt, Eastern Goldfields Province, Western Australia, *Precambrian Res.*, 48, 63-73.

Thompson, A.B. (1984), Geothermal gradients through time, in *Patterns of Change in Earth Evolution*, edited by H.D. Holland and A. F. Trendall, pp. 345-355, Springer-Verlag, Berlin.

Thurston, P.C. (2002), Autochthonous development of Superior Province greenstone belts?, *Precambrian Res.*, 105, 11-36.

Tomlinson, K.Y., D.W. Davis, D. Stone, and T.R. Hart (2003), U-Pb age and Nd isotopic evidence for Archean terrane development and crustal recycling in the south-central Wabigoon subprovince, Canada, *Contrib. Mineral. Petrol.*, 144, 684-702.

van der Molen, I., and M.S. Paterson (1979), Experimental deformation of partially-melted granite, *Contrib. Mineral. Petrol.*, 70, 299-318.

Van Kranendonk, M.J., W.J. Collins, A.H. Hickman, and M.J. Pawley (2004), Critical tests of vertical vs. horizontal tectonic models for the Archaean East Pilbara Granite-Greenstone Terrane, Pilbara Craton, Western Australia, *Precambrian Res.*, 131, 173-211.

Van Kranendonk, M.J., A.H. Hickman, R.H. Smithies, D.R. Nelson, and G. Pike (2002), Geology and tectonic evolution of the Archean North Pilbara Terrain, Pilbara Craton, Western Australia, *Econ. Geol.*, 97, 695-732.

Weinberg, R.F., L. Moresi, and P. van der Borgh (2003), Timing of deformation in the Norseman-Wiluna Belt, Yilgarn Craton, Western Australia, *Precambrian Res.*, 120, 219-239.

Weinberg, R.F., and Y. Podladchikov (1994), Diapiric ascent of magmas through power law crust and mantle, *J. Geophys. Res.*, 99, 9543-9959.

Wellman, P. (2000), Upper crust of the Pilbara Craton, Australia: 3D geometry of a granite/greenstone terrain, *Precambrian Res.*, 104, 175-186.

West, G.F., and J.-C. Mareschal (1979), A model for Archean tectonism. Part 1. The thermal conditions, *Can. J. Earth Sci.*, 16, 1942-1950.

White, D.J., G. Musacchio, H.H. Helmstaedt, R.M. Harrap, P.C. Thurston, A. van der Velden, and K. Hall (2003), Images of a lower-crustal oceanic slab: direct evidence for tectonic accretion in the Archean western Superior Province, *Geology*, 31, 997–1000.

Williams, I.S., and W.J. Collins (1990), Granite-greenstone terranes in the Pilbara Block, Australia, as coeval volcano-plutonic complexes; evidence from U-Pb zircon dating of the Mount Edgar Batholith, *Earth Planet. Sci. Lett.*, 97, 41-53.

Wolf, M.B., and P.J. Wyllie (1993), Garnet growth during amphibolite anatexis: implications of a garnetiferous restite, *J. Geol.*, 101, 357-373.

Wyllie, P.J., M.B. Wolf, and S.R. van der Laan (1997), Conditions for formation of tonalites and trondhjemites: magmatic sources and products, in *Greenstone Belts*, edited by M.J. de Wit and L.D. Ashwal, pp. 256-266, Clarendon Press, Oxford.

Zegers, T.E. (2004), Granite formation and emplacement as indicators of Archaean tectonic processes, in *The Precambrian Earth: Tempos and Events*, edited by P.G. Eriksson, W. Altermann, D.R. Nelson, W. U. Mueller, and O. Catuneanu, pp. 103-118, Elsevier, Amsterdam.

Zegers, T.E., S.E. White, M. de Keijzer, and P. Dirks (1996), Extensional structures during deposition of the 3460 Ma Warrawoona Group in the eastern Pilbara Craton, Western Australia, *Precambrian Res.*, 80, 89-105.

S. Bodorkos, Geological Survey of Western Australia, 100 Plain Street, East Perth, Western Australia 6004, Australia. simon.bodorkos@doir.wa.gov.au

M. Sandiford, School of Earth Sciences, University of Melbourne, Melbourne, Victoria 3010, Australia. mikes@unimelb.edu.au